

Stationary states and quantum quench dynamics of Bose-Einstein condensates in a double-well potential

Linghua Wen,^{1,*} Qizhong Zhu,² Tianfu Xu,¹ Xili Jing,¹ and Chengshi Liu¹

¹*College of Science, Yanshan University, Qinhuangdao 066004, China*

²*Department of Physics and Center of Theoretical and Computational Physics,
The University of Hong Kong, Hong Kong, China*

(Dated: June 10, 2022)

We consider the properties of stationary states and the dynamics of Bose-Einstein condensates (BECs) in a double-well (DW) potential with pair tunneling by using a full quantum-mechanical treatment. Furthermore, we study the quantum quench dynamics of the DW system subjected to a sudden change of the Peierls phase. It is shown that strong pair tunneling evidently influences the energy spectrum structure of the stationary states. For relatively weak repulsive interatomic interactions, the dynamics of the DW system with a maximal initial population difference evolves from Josephson oscillations to quantum self-trapping as one increases the pair tunneling strength, while for large repulsion the strong pair tunneling inhibits the quantum self-trapping. In the case of attractive interatomic interactions, strong pair tunneling tends to destroy the Josephson oscillations and quantum self-trapping, and the system eventually enters a symmetric regime of zero population difference. Finally, the effect of the Peierls phase on the quantum quench dynamics of the system is analyzed and discussed. These new features are remarkably different from the usual dynamical behaviors of a BEC in a DW potential.

PACS numbers: 05.30.Jp, 03.75.Lm, 67.85.Bc

I. INTRODUCTION

Stationary state properties and dynamics of ultracold atoms in a double-well (DW) potential have attracted considerable attention over the past few decades [1, 2]. As a powerful building block model, the double well plays a key role in revealing numerous interesting phenomena of quantum many-body and few-body systems due to the experimental accessibility and precise controllability. Actually, many intriguing properties have been predicted theoretically and some observed experimentally in Bose-Einstein condensates (BECs) or ultracold fermionic atoms in a DW potential, ranging from the Josephson effect and quantum self-trapping [3–14], fragmentation of a BEC [15, 16], entangled clusters [17] and NOON-like states [18] of condensed bosons, quantum chaos [19], hidden vortices [20, 21] and vortex superpositions [22], and spin correlation [23] to two-particle analog of a charge-density-wave state [24], etc. Of particular interest is the quantum tunneling dynamics in a DW BEC because it represents one of the most surprising and paradigmatic effects in quantum mechanics. Although tunneling is a fundamental phenomenon in wave dynamics (for instance, the dynamics of atomic matter waves and the classical dynamics of optical waves) [25], the quantum tunneling of ultracold bosonic atoms through a potential barrier between two wells provides a direct manifestation of quantum phase coherence. Recently, a correlated quantum tunneling was observed in Ref. [26] and a relevant theoretical analysis was pre-

sented by means of two-body dynamics [27]. Further study demonstrates that correlated tunneling is principally resulted from pair tunneling, which involves the superexchange interactions between particles on neighboring wells [28]. Most recently, spontaneous symmetry breaking and effective ground state in a DW BEC with pair tunneling are discussed in Ref. [29]. These theoretical investigations [27–29] concerning to the pair tunneling are confined to the regime of repulsive interatomic interactions. In addition, the analyses in Refs. [27, 28] are illustrated with a two-atom or few-body system. However, the usual realistic ultracold atomic gases in experiments should be many-body systems. In fact, strong many-body effect may basically alter the tunneling configuration of the DW system.

On the other hand, the research on neutral atoms in synthetic gauge fields has become an active new subject in the filed of cold atom physics [30]. The artificial gauge potentials constitute novel tools for exploring the properties of ultracold atoms, which usually occur in the field of condensed matter physics. Recently, Spielman's group experimentally realized a Peierls substitution for ultracold neutral atoms in an artificial lattice potential [31], where the Peierls phase can be controlled precisely. The effective vector gauge potential is characterized by a complex tunneling parameter $J = |J|e^{i\theta}$, where θ is the so-called Peierls phase gained by an atom tunneling from site $j + 1$ to j . In addition, the Peierls phase may also be created in a shaken optical lattice [32, 33] or a spin-dependent optical lattice [34]. In these studies, the equilibrium states of the many-body system can be well described. However, little is known about the quantum quench dynamics of a system far from equilibrium, especially for the quantum quenches of the Hamiltonian

*Electronic address: linghuawen@ysu.edu.cn

caused by a sudden change of the Peierls phase. From a fundamental viewpoint, the quantum quench dynamics of cold atom systems far from equilibrium is very interesting because it can reveal rich properties of the many-body system beyond ground state. For instance, *Zitterbewegung* oscillation and dynamical topological phases have been observed most recently in a quenched spin-orbit-coupled (SOC) BEC [35] and a quenched SOC degenerate Fermi gas [36], respectively.

In this work we investigate the stationary state properties of a BEC in a DW potential with pair tunneling and the quantum dynamics of the DW system with a maximal initial population difference as well as the quench dynamics of the system by abruptly changing the Peierls phase. Although the problems of bosons in a DW potential can be solved under certain conditions by several semi-classical analytical approximations, such as mean-field theory [3, 4, 7], variational approach to many-body ground state [15], phase-space analysis of many-body bosons [11, 19] and WKB approach [9], these semi-classical treatments are usually too complicated and redundant in understanding the physical essence of the problems. In particular, the correlated tunneling observed in Ref. [26] can not be described by the standard Bose-Hubbard (BH) Hamiltonian [37] based on the hard-core interaction under the semi-classical approximations. Here we adopt a tractable full quantum-mechanical scheme to tackle the present problem. The main features are summarized as follows. First, strong pair tunneling can make the eigenstates of the system evolves from delocalized states to Schrödinger cat-like states and quantum self-trapping states and vice versa, depending on the many-body interactions. Second, for the case of relatively weak repulsive interactions strong pair tunneling sustains a quantum self-trapping, but for the case of large repulsive interactions the strong pair tunneling tends to destroy the self-trapping. On the other hand, for attractive interatomic interactions the strong pair tunneling tends to eliminate the Josephson oscillation and quantum self-trapping irrespective of the interaction strength. Finally, once the DW system is quenched, the population difference shows evident oscillation behaviors for most cases. The maximum oscillation amplitude is directly relevant to the value of the Peierls phase. These interesting features are markedly different from the usual stationary state structures and dynamical behaviors of a BEC in a DW potential, which allows to be observed and tested under current experimental technique conditions.

The paper is organized as follows. In Sec. II, the model Hamiltonian is introduced. The general properties of the stationary states of the system are described in Sec. III. The dynamics of the system with a maximal initial population difference is investigated in Sec. IV. The quantum quench dynamics of the DW system is discussed in Sec. V. Conclusions are outlined in Sec. VI.

II. MODEL

We consider a system of N ultracold bosonic atoms in a DW potential. At low temperatures the second-quantized Hamiltonian of the system beyond the onsite approximation can be written as [28, 29, 31, 38, 39]

$$\begin{aligned} \hat{H} = & -[J - U_3(\hat{n}_1 + \hat{n}_2 - 1)] \left(e^{i\theta} \hat{a}_1^\dagger \hat{a}_2 + e^{-i\theta} \hat{a}_2^\dagger \hat{a}_1 \right) \\ & + \frac{U_0}{2} \left(\hat{a}_1^\dagger \hat{a}_1^\dagger \hat{a}_1 \hat{a}_1 + \hat{a}_2^\dagger \hat{a}_2^\dagger \hat{a}_2 \hat{a}_2 \right) + (U_1 + U_2) \hat{n}_1 \hat{n}_2 \\ & + \frac{U_2}{2} \left(e^{2i\theta} \hat{a}_1^\dagger \hat{a}_1^\dagger \hat{a}_2 \hat{a}_2 + e^{-2i\theta} \hat{a}_2^\dagger \hat{a}_2^\dagger \hat{a}_1 \hat{a}_1 \right) \\ & + \mu(\hat{n}_1 - \hat{n}_2), \end{aligned} \quad (1)$$

where $\hat{n}_j = \hat{a}_j^\dagger \hat{a}_j$ and \hat{a}_j (\hat{a}_j^\dagger) is the bosonic annihilation (creation) operator for well j . J is the hopping amplitude of single-particle tunneling, U_0 is the on-site two-body interaction strength, U_1 is the inter-well particle interaction, U_2 describes the atom-pair tunneling (pair tunneling), and U_3 denotes the density-dependent tunneling [28, 29, 39]. θ represents a tunable Peierls phase [31], and the tilt parameter μ denotes the difference of local chemical potentials caused for instance by a mismatch between the two wells. In general, $U_1 \approx U_2$, and the coupling constants U_1 , U_2 , and U_3 are smaller compared with U_0 . Throughout this paper we assume $U_1 = U_2$ for the DW system and take $U_3 \approx 2.5U_2$, which is consistent with the choice of the corresponding parameters in Ref. [26, 28]. When $\theta = 0$ and the terms involving U_1 , U_2 , and U_3 are neglected, equation (1) becomes the standard BH Hamiltonian for a DW potential [37, 39].

By introducing the notations $\hat{H}_r = \hat{H}/NJ$, $\tilde{U}_0 = NU_0/2J$, $\tilde{U}_2 = NU_2/2J$, $\tilde{U}_3 = NU_3/2J$, and $\tilde{\mu} = \mu/J$, we obtain the rescaled Hamiltonian in reduced units

$$\begin{aligned} \hat{H}_r = & - \left[\frac{1}{N} - \frac{2\tilde{U}_3}{N^2} (\hat{n}_1 + \hat{n}_2 - 1) \right] \left(e^{i\theta} \hat{a}_1^\dagger \hat{a}_2 + e^{-i\theta} \hat{a}_2^\dagger \hat{a}_1 \right) \\ & + \frac{\tilde{U}_0}{N^2} \left(\hat{a}_1^\dagger \hat{a}_1^\dagger \hat{a}_1 \hat{a}_1 + \hat{a}_2^\dagger \hat{a}_2^\dagger \hat{a}_2 \hat{a}_2 \right) + \frac{4\tilde{U}_2}{N^2} \hat{n}_1 \hat{n}_2 \\ & + \frac{\tilde{U}_2}{N^2} \left(e^{2i\theta} \hat{a}_1^\dagger \hat{a}_1^\dagger \hat{a}_2 \hat{a}_2 + e^{-2i\theta} \hat{a}_2^\dagger \hat{a}_2^\dagger \hat{a}_1 \hat{a}_1 \right) \\ & + \frac{\tilde{\mu}}{N} (\hat{n}_1 - \hat{n}_2), \end{aligned} \quad (2)$$

where the tilde is omitted for simplicity. The most general N -body state vector is a linear superposition of Fock states

$$|\psi\rangle = \sum_{k=1}^{N+1} c_k |k-1, N-k+1\rangle, \quad (3)$$

with $k-1$ being the occupation number corresponding to the left well and

$$|k-1, N-k+1\rangle = \frac{e^{i(k-1)\theta} \left(\hat{a}_1^\dagger \right)^{k-1} \left(\hat{a}_2^\dagger \right)^{N-k+1}}{\sqrt{(k-1)! (N-k+1)!}} |vac\rangle. \quad (4)$$

The number of atoms in the j th well is $N_j = \langle \psi | \hat{a}_j^\dagger \hat{a}_j | \psi \rangle$, $N = N_1 + N_2$ is the total number of atoms, and the population difference is defined as $z = (N_1 - N_2)/N$. The generic properties of the stationary states of the system can be obtained by solving the eigenvalue equation of the Hamiltonian (2).

The dynamics of the system is described by the time-dependent Schrödinger equation

$$\frac{i}{N} \frac{\partial}{\partial \tau} |\Psi\rangle = \hat{H}_\tau |\Psi\rangle, \quad (5)$$

where the time is measured in tunneling time units: $\tau = t/T$ with $T = \hbar/J$. The time-dependent solution of equation (5) can be expanded in the Fock basis

$$|\Psi(\tau)\rangle = \sum_{k=1}^{N+1} C_k(\tau) |k-1, N-k+1\rangle. \quad (6)$$

Combining equations (5) and (6), we can obtain the coupled equations for the time evolution of the coefficients C_k

$$\begin{aligned} \frac{i}{N} \frac{d}{d\tau} C_1 &= \left[U_0 \left(1 - \frac{1}{N} \right) - \mu \right] C_1 \\ &+ \left[\frac{2U_3(N-1)}{N^{3/2}} - \frac{1}{\sqrt{N}} \right] e^{-i\theta} C_2 \\ &+ \frac{U_2 \sqrt{2N(N-1)}}{N^2} e^{-2i\theta} C_3, \end{aligned} \quad (7)$$

$$\begin{aligned} \frac{i}{N} \frac{d}{d\tau} C_2 &= \frac{U_0(N-1)(N-2) + 4U_2(N-1)}{N^2} C_2 \\ &+ \mu \left(\frac{2}{N} - 1 \right) C_2 \\ &+ \frac{2U_3(N-1) - N}{N^{3/2}} e^{i\theta} C_1 \\ &+ \frac{[2U_3(N-1) - N] \sqrt{2(N-1)}}{N^2} e^{-i\theta} C_3 \\ &+ \frac{U_2 \sqrt{6(N-1)(N-2)}}{N^2} e^{-2i\theta} C_4, \end{aligned} \quad (8)$$

$$\begin{aligned} \frac{i}{N} \frac{d}{d\tau} C_k &= a_k C_k + b_{k-1} e^{i\theta} C_{k-1} + b_{k+1} e^{-i\theta} C_{k+1} \\ &+ d_{k-2} e^{2i\theta} C_{k-2} + d_{k+2} e^{-2i\theta} C_{k+2}, \\ &(k = 3, 4, \dots, N-1), \end{aligned} \quad (9)$$

$$\begin{aligned} \frac{i}{N} \frac{d}{d\tau} C_N &= \frac{U_0(N-1)(N-2) + 4U_2(N-1)}{N^2} C_N \\ &+ \mu \left(1 - \frac{2}{N} \right) C_N \\ &+ \frac{[2U_3(N-1) - N] \sqrt{2(N-1)}}{N^2} e^{i\theta} C_{N-1} \\ &+ \frac{2U_3(N-1) - N}{N^{3/2}} e^{-i\theta} C_{N+1} \\ &+ \frac{U_2 \sqrt{6(N-1)(N-2)}}{N^2} e^{2i\theta} C_{N-2}, \end{aligned} \quad (10)$$

$$\begin{aligned} \frac{i}{N} \frac{d}{d\tau} C_{N+1} &= \left[U_0 \left(1 - \frac{1}{N} \right) + \mu \right] C_{N+1} \\ &+ \frac{U_2 \sqrt{2N(N-1)}}{N^2} e^{2i\theta} C_{N-1} \\ &+ \frac{2U_3(N-1) - N}{N^{3/2}} e^{i\theta} C_N, \end{aligned} \quad (11)$$

where $a_k = (U_0/N^2)[(k-1)(k-2) + (N-k)(N-k+1)] + (4U_2/N^2)(k-1)(N-k+1) + (\mu/N)[2(k-1) - N]$, $b_{k-1} = [2U_3(N-1)/N^2 - 1/N] \sqrt{(k-1)(N-k+2)}$, $b_{k+1} = [2U_3(N-1)/N^2 - 1/N] \sqrt{k(N-k+1)}$, $d_{k-2} = (U_2/N^2) \sqrt{(k-1)(k-2)(N-k+2)(N-k+3)}$, and $d_{k+2} = (U_2/N^2) \sqrt{k(k+1)(N-k)(N-k+1)}$. The time-dependent population difference between the left and right wells is given by

$$z(\tau) = \frac{\sum_{k=1}^{N+1} (2k - N - 2) |C_k(\tau)|^2}{N}, \quad (12)$$

where the coefficients are normalized as $\sum_{k=1}^{N+1} |C_k(\tau)| = 1$.

In the following we systematically investigate the general properties of the stationary states of the DW system with pair tunneling both for repulsive and attractive interatomic interactions. Moreover, we discuss the dynamics of the system with a maximal initial population imbalance. Finally, we analyze the quantum quench dynamics of the system by suddenly changing the value of the Peierls phase at a certain moment.

III. PROPERTIES OF THE STATIONARY STATES OF THE DW SYSTEM WITH PAIR TUNNELING

We first consider the stationary state properties of the DW system. The eigenstates can be obtained through the exact diagonalization [11] of the Hamiltonian (2) in the $(N+1)$ -dimensional space spanned by the Fock basis: $\{|0, N\rangle, |1, N-1\rangle, \dots, |N-1, 1\rangle, |N, 0\rangle\}$. In figure 1, we show the density profiles $|c_k^s|^2$ of the eigenvector of the Hamiltonian (2) for various parameters, where $N = 50$, $\theta = 0$, and $s = 1, 2, \dots, N+1$ denotes the ordinal number of the eigenvector ordered by increasing eigenvalue. For the case of $U_0 = 0$, $U_2 = 0$, and $\mu = 0$ (i.e., there is no interatomic interaction and the double well is symmetric), the density profile of each eigenstate displays excellent left-right symmetry [figure 1(a1)], where the eigenstates are non-degenerate. With the increasing of the interatomic interaction, the high-lying excited states gradually form degenerate pairs according to the up-down order. The degeneracy of each pair in the excited states can be eliminated by artificially introducing a small tilt of the double well. We show that for a repulsive interatomic interaction U_0 above a critical value the left-right symmetry of the high-lying states is broken such that

the density profile develops an evident population imbalance and occupies mainly one region of the Fock space. Consequently, the highest excited state spontaneously acquires a large population imbalance, which means the highest-lying state evolves from a delocalized state to a Schrödinger cat-like state and eventually to a quantum self-trapping state due to the symmetry breaking. The above analysis can explain why there is a large dropwell of the density profiles in figure 1(a2). When the repulsive interaction U_0 is sufficiently strong, the density profiles become almost two cross line segments [figure 1(a3)]. In this situation, most energy eigenstates are pair quasi-degenerate and non-extended (cat-like or highly localized). Physically, this point can be understood because the sufficiently strong repulsive interaction is equivalent to a very high central barrier of the DW potential, where the particle tunneling between the two wells is highly suppressed and the coherence between the two sites is lost. For the case of ground state, a well-known paradigm is the Mott insulator phase with a commensurating filling in a optical lattice [37, 40]. Note that the case of attractive interactions is similar to that of the repulsive interactions, but the role played by the highest-lying excited state is now replaced by the ground state of the Hamiltonian (2) and the low-lying eigenstates exhibit two-fold degeneracy [see figure 3(b)].

In the meantime, we find that the density profiles of the stationary states are significantly influenced by the pair tunneling and the tilt parameter of the DW potential. For weak repulsive interaction as well as weak pair tunneling, the density distributions are similar to those in figure 1(a1) except for a further broadening in the upper region [figure 1(b1)]. However, for large repulsive interaction, pair tunneling exhibits distinct effect on the density profiles, as shown in figures 1(b2) and 1(b3). Essentially, the single-particle Josephson tunneling is suppressed for strong repulsion and the pair tunneling gradually becomes dominant with continuously increasing interactions. As mentioned above, the coupling constant $U_3 = 2.5U_2$ is in direct proportion to the pair tunneling. In the case of $U_0 = 10$ and $U_2 = 0.02U_0$, the term of $2U_3(\hat{n}_1 + \hat{n}_2 - 1)/N^2$ in equation (2) actually suppresses the interwell hopping. Thus the pair tunneling tends to make the eigenstates more localized in comparison with the case of $U_0 = 10$ and $U_2 = 0$, which can be seen in figure 1(b2). In addition, the effective single-atom Josephson tunneling constant $(1/N - 2U_3(N - 1)/N^2)$ can become a negative value for sufficiently large U_3 (i.e., for sufficiently large pair tunneling U_2 according to the relation $U_3 = 2.5U_2$). Consequently, for the case of superstrong interaction $U_0 = 500$, the pair tunneling $U_2 = 0.02U_0$ does not make the eigenstates further localized but more extended instead [see figure 1(b3)]. The effect of the bias of the double well on the density profiles is shown in figures 1(c1)-1(c3). When $\mu > 0$ and $U_0 > 0$, the density profiles of the low-lying states display a shift towards the left side and those of the high-lying states keep only the right branch [figure 1(c1)] due to the sym-

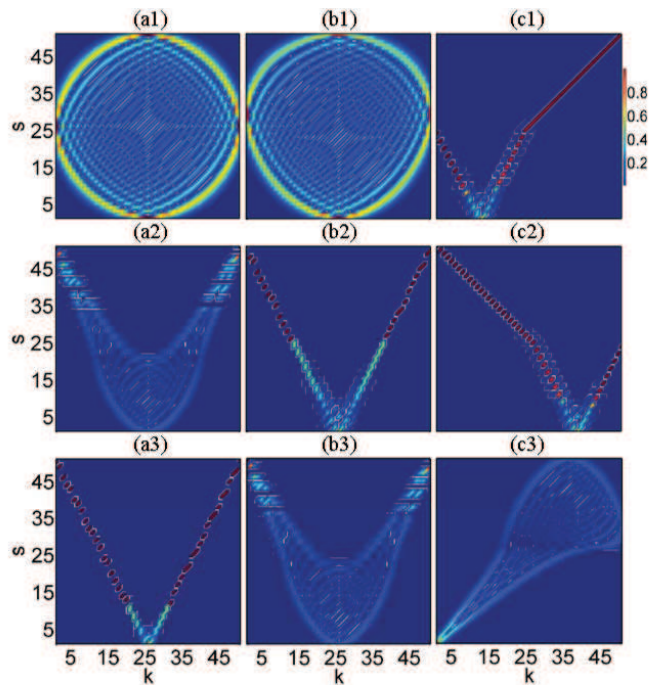


FIG. 1: (color online) Density profiles $|c_k^s|^2$, where $k = 1, 2, \dots, N + 1$, and the ordinal number of the energy eigenstate $s = 1, 2, \dots, N + 1$. (a1) $U_0 = 0, U_2 = 0, \mu = 0$, (a2) $U_0 = 10, U_2 = 0, \mu = 0$, (a3) $U_0 = 500, U_2 = 0, \mu = 0$, (b1) $U_0 = 0.5, U_2 = 0.02U_0, \mu = 0$, (b2) $U_0 = 10, U_2 = 0.02U_0, \mu = 0$, (b3) $U_0 = 500, U_2 = 0.02U_0, \mu = 0$, (c1) $U_0 = 10, U_2 = 0.02U_0, \mu = 5$, (c2) $U_0 = 10, U_2 = 0.02U_0, \mu = -5$, and (c3) $U_0 = -10, U_2 = 0.02U_0, \mu = 5$. Here $\theta = 0$ and $N = 50$.

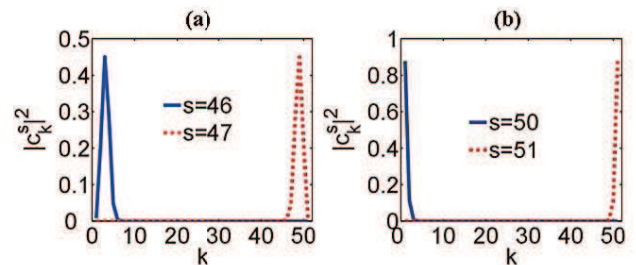


FIG. 2: (color online) Density profiles $|c_k^s|^2$ for typical degenerate eigenstate pairs in figure 1(a2). (a) The 46th eigenstate (solid blue line) and the 47th eigenstate (dashed red line), and (b) the 50th eigenstate (solid blue line) and the 51st eigenstate (dashed red line). The distributions of these high-lying states are strongly localized in the Fock space.

metry breaking of the left-right wells, while the case is reversed when $\mu < 0$ and $U_0 > 0$ [figure 1(c2)]. Furthermore, the combining effect of attractive interaction and pair tunneling as well as the bias of the DW potential is demonstrated in figure 1(c3).

Figure 2 shows the density profiles $|c_k^s|^2$ for the 46th, 47th, 50th, and 51st eigenstates in figure 1(a2), where the former two states and the latter ones are two-fold degenerate, respectively. Obviously, these high-lying excited

states are strongly localized in the Fock space. In the absence of pair tunneling, a dynamical quantum phase transition from the Josephson regime to the self-trapped regime in a DW BEC has been discussed recently in Ref. [11].

In figure 3, we present the lowest nine (ten) eigenvalues of the DW system for repulsive (attractive) interatomic interaction as a function of the ratio $r = U_2/[N - 2U_3(N - 1)]$ between the pair tunneling strength and the single-particle tunneling strength, where $N = 50$, $\mu = 0$, and $\theta = 0$. It is shown that for strong repulsive interaction $U_0 = 100$ and zero pair tunneling the lowest seven eigenstates are non-degenerate and pair degeneracy occurs from the eighth eigenstate [figure 3(a)]. With the increasing of r (i.e., with the increasing of pair tunneling) below a critical value $r_c = 0.2$ the energy gap between two nearest-neighbor non-degenerate eigenstates decreases remarkably. However, with the further increase of r the energy levels almost keep constant and exhibit a characteristic of degeneracy or quasi-degeneracy. By contrast, for attractive interaction the lowest ten eigenstates are pair degeneracy (or quasi-degeneracy) irrespective of the pair tunneling strength, where the relations between E and r are similar to those in figure 3(a). Physically, the degeneracy or quasi-degeneracy of the energy levels are resulted from the interatomic interactions (including the on-site two-body interaction, the inter-well particle interaction, and the pair tunneling). According to the definition of the tunneling ratio r , the pair tunneling strength can be expressed by $U_2 = N/[1/r + 5(N - 1)]$ because of $U_3 = 2.5U_2$. When $r > r_c$, the pair tunneling strength U_2 approaches an asymptotic value $N/5(N - 1)$. Therefore with the further increase of r the eigenenergies of the system tend to keep constant, which can be seen in the reduced Hamiltonian of equation (2). The present results indicate that the stability of the ground state (both for repulsive and attractive interactions) is not affected basically by the tunneling ratio r as long as it is not less than a critical value.

Here we find that the Peierls phase θ does not influence the stationary energy spectrums and the density profiles of the eigenvectors of the DW system. This can be understood in terms of the expressions of the Hamiltonian (1) and the Fock states (4). If we make a gauge transformation $e^{i\theta}\hat{a}_1^\dagger \rightarrow \hat{a}_1^\dagger$, equation (1) reduces to the Hamiltonian of the DW system without terms of Peierls phase.

IV. QUANTUM DYNAMICS OF THE DW SYSTEM WITH A MAXIMAL INITIAL POPULATION DIFFERENCE

Next, we analyze the quantum dynamics of the DW system with a maximal initial population difference $z(0) = 1$ and $|\Psi(0)\rangle = |N, 0\rangle$. We numerically solve the coupled equations (7)-(11) using the fourth-order Runge-Kutta method. The most important physical quantity characterizing the tunneling dynamics and quantum fluc-

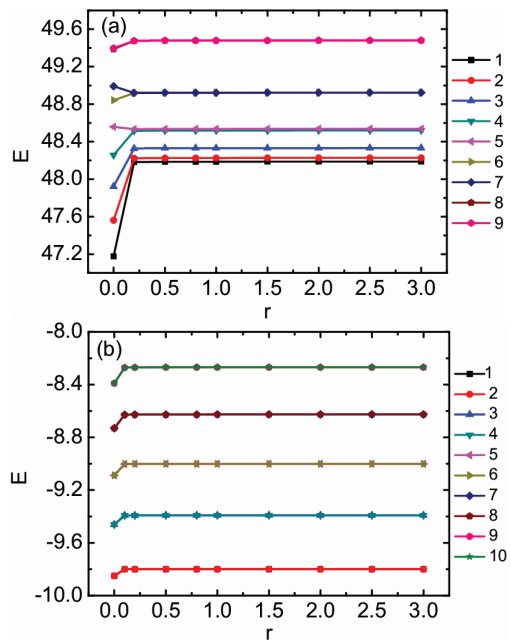


FIG. 3: (color online) (a) The lowest nine energy levels (1–9) as a function of the ratio r between the pair tunneling strength and the single-particle tunneling strength, where the relevant parameters are $U_0 = 100$, $N = 50$, $\mu = 0$, and $\theta = 0$. (b) The lowest ten energy levels (1–10) as a function of the ratio r . The parameters are $U_0 = -10$, $N = 50$, $\mu = 0$, and $\theta = 0$.

tuations of the DW system is the population difference. For the case of non-interacting limit and symmetric DW potential, the system consists of N independent particles and thus the evolution of the population difference yields an obvious Rabi oscillation [3, 4, 7, 11], which can be seen in figure 4(a1). In the presence of the bias of the double well, the population difference exhibits a damped oscillation and finally approaches a large steady value due to the incommensurate tunneling between the two wells [figure 4(a2)]. In the typical Josephson regime (for instance, $U_0 = 1.2$, $U_2 = 0$, $\mu = 0$), the evolution of the population difference always shows damping oscillations followed by complex revivals as shown in figure 4(a3). When the repulsive interatomic interaction, e.g., $U_0 = 4$, is larger than a critical value, the population difference undergoes a damped oscillation and then keeps a positive constant, which indicates that the system is in a quantum self-trapping state [see figure 4(a4)]. For the case of repulsive interactions, the quantum self-trapping effect is directly related to the properties of the highest-lying state of the system Hamiltonian (2). As a matter of fact, when the initial quantum state is prepared with strong repulsion U_0 above a critical value and with large population difference, the system will remain trapped due to the large overlap of the initial state with the highest excited state of the system.

Not only does the pair tunneling influence remarkably the structure of the stationary states but also the

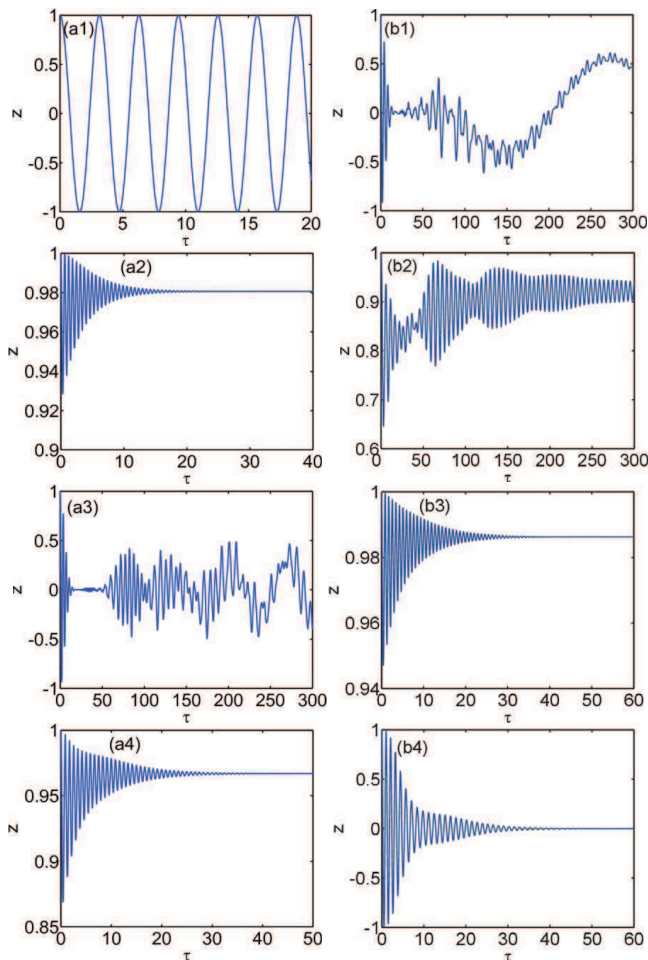


FIG. 4: (color online) Time evolution of the population difference for a quantum state of the DW system initially prepared with $|\Psi(0)\rangle = |N, 0\rangle$ and $z(0) = 1$. (a1) $U_0 = 0$, $U_2 = 0$, $\mu = 0$, (a2) $U_0 = 0$, $U_2 = 0$, $\mu = 5$, (a3) $U_0 = 1.2$, $U_2 = 0$, $\mu = 0$, (a4) $U_0 = 4$, $U_2 = 0$, $\mu = 0$, (b1) $U_0 = 1.2$, $U_2 = 0.02U_0$, $\mu = 0$, (b2) $U_0 = 1.2$, $U_2 = 0.2U_0$, $\mu = 0$, (b3) $U_0 = 4$, $U_2 = 0.02U_0$, $\mu = 0$, and (b4) $U_0 = 4$, $U_2 = 0.2U_0$, $\mu = 0$. The Peierls phase is $\theta = 0$. Here the horizontal ordinate τ is in units of \hbar/J .

quantum dynamics of the DW system. In the case of $U_0 = 1.2$, $U_2 = 0.02U_0$ and $\mu = 0$, the revival-collapse-revival evolution in the Josephson regime becomes a modulated S-like oscillation as shown in figures 4(b1) and 4(a3), which leads to a significant modification of the dynamics. When the pair tunneling strength increases to $U_2 = 0.2U_0$ (strong pair tunneling), the population difference oscillates anharmonically around an increasing time averaged value of $\langle z(\tau) \rangle \neq 0$. During the long-time evolution of $z(\tau)$, the oscillation amplitude gradually decreases and finally the population difference tends to keep a positive constant value [figure 4(b2)]. Here the intriguing self-trapping phenomenon is essentially resulted from the strong pair tunneling. For larger interatomic interaction $U_0 = 4$, the medium strength pair tunneling $U_2 = 0.02U_0$ makes the oscillating population difference

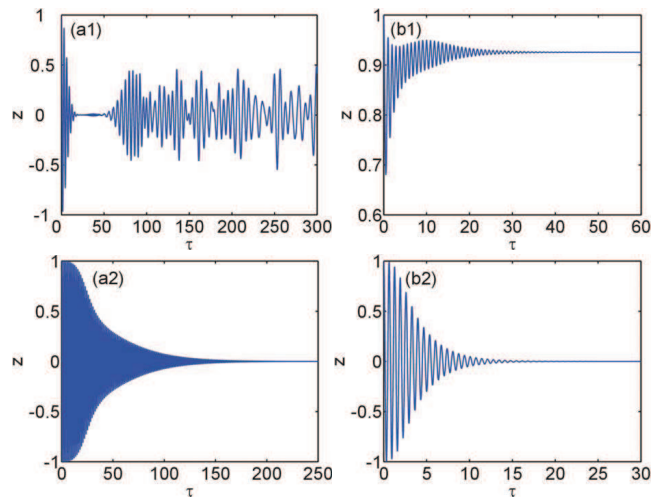


FIG. 5: (color online) Time evolution of the population difference for a quantum state of the DW system initially prepared with $|\Psi(0)\rangle = |N, 0\rangle$ and $z(0) = 1$. (a1) $U_0 = -1.2$, $U_2 = 0.02U_0$, (a2) $U_0 = -1.2$, $U_2 = 0.2U_0$, (b1) $U_0 = -4$, $U_2 = 0.02U_0$, and (b2) $U_0 = -4$, $U_2 = 0.2U_0$. The other parameters are $\mu = 0$ and $\theta = 0$. Here the horizontal ordinate τ is in units of \hbar/J .

decay to a higher constant value, which implies that weak and medium pair tunnelings will significantly enhance the quantum self-trapping effect in a DW system [figure 4(b3)]. By contrast, the strong pair tunneling $U_2 = 0.2U_0$ does not strengthen the quantum self-trapping in the case of large repulsion, but it destroys fully the self-trapping effect instead because of the final zero population difference [figure 4(b4)]. From the foregoing analysis, we can conclude that for the case of weak repulsion the strong pair tunneling sustains a quantum self-trapping while for the case of large repulsion the strong pair tunneling tends to destroy the quantum self-trapping effect.

Figure 5 displays the evolution of population difference for a DW system with attractive interatomic interactions and pair tunneling, where $\mu = 0$, $\theta = 0$, and the initial state of the system is $|\Psi(0)\rangle = |N, 0\rangle$ and $z(0) = 1$. In the case of $U_0 = -1.2$ and $U_2 = 0.02U_0$ (weak attractive interaction and medium strength pair tunneling), the population difference shows modulated Josephson oscillations [figure 5(a1)], which is, to a certain extent, similar to those in figures 4(a3) and 4(b1). For $U_0 = -4$ and $U_2 = 0.02U_0$, the system exhibits obvious self-trapping behavior as shown in figure 5(b1). In particular, we find that strong pair tunneling thoroughly eliminates the self-trapping phenomenon in the DW system for both weak and strong attractive interactions, where the ultimate population difference remains zero [figures 5(a2) and 5(b2)]. Note that the shade region in figure 5(a2) represents rapid oscillations of the population difference.

V. QUANTUM QUENCH DYNAMICS OF THE DW SYSTEM IN THE PRESENCE OF PAIR TUNNELING

Now we discuss the quantum quench dynamics of the DW system so that we can explore the effect of the Peierls phase on the dynamic properties of the system. We say that the system is quenched if the Peierls phase θ is changed suddenly at a certain moment from one value to another. For simplicity, suppose that at the initial time $\tau = 0$ the DW system is quenched by changing the value of θ from zero to a nonzero constant value and the initial state $|\Psi(0)\rangle$ is the ground state of the DW system with $\theta = 0$. In order to ensure the accuracy and reliability, we test in advance the dynamical evolution of the ground state of the DW system before computing the quench dynamics of the system for each given set of parameters. The reasonable time-dependent population difference concerning the dynamics of the ground state of the system should be a perfect straight line, which has been verified in our simulations.

Figure 6 shows the quench dynamics of the DW system for repulsive interatomic interactions, where $N = 50$, $\mu = 0$, and $U_2/U_0 = 0.002$. For $0 < \theta < \pi$, the larger the value of θ is, the larger the maximum amplitude of the oscillation becomes, and at the same time the shorter the quasi-period of collapse and revival gets. The case is reversed for $\pi < \theta < 2\pi$ (not shown here). In addition, for the same Peierls phase θ , the stronger the repulsive interaction is, the lower the maximum amplitude of the oscillation is. This feature can be understood because the large interatomic interaction is equivalent to a high potential barrier which weakens the particle tunneling and tends to make the atoms localized. We show that for repulsive interactions and $\theta = \pi$ there exists no oscillation behavior during the dynamic evolution of the DW system and the population difference keeps unchanged, i.e., $z(\tau) = 0$. The main reason is that the ground state of the system with $\theta = 0$ (i.e., the initial state) in the case of repulsive interatomic interactions is always symmetric and thus a π Peierls phase does not influence the single-particle tunneling and the pair tunneling as shown in equations (1) and (2).

In the case of attractive interatomic interactions, the quantum quench dynamics of the system becomes more complicated. For weak attractive interaction $U_0 = -2$ (Josephson oscillation regime), the oscillation is somewhat erratic as shown in figures 7(a1) and 7(a2). Physically, particle number fluctuations can automatically admit the excited states of the system due to the many-body interactions. Thus the quench caused by the sudden change of the Peierls phase generates various elementary excitations with different frequencies. The similar feature is also found in the case of few-bosons dynamics in a double well [27]. With the time evolution, the population difference finally restores to its initial value $z = 0$. From figures 7(a1) and 7(a2), one can see that when the Peierls phase θ ($0 < \theta < \pi$) get larger the maximum

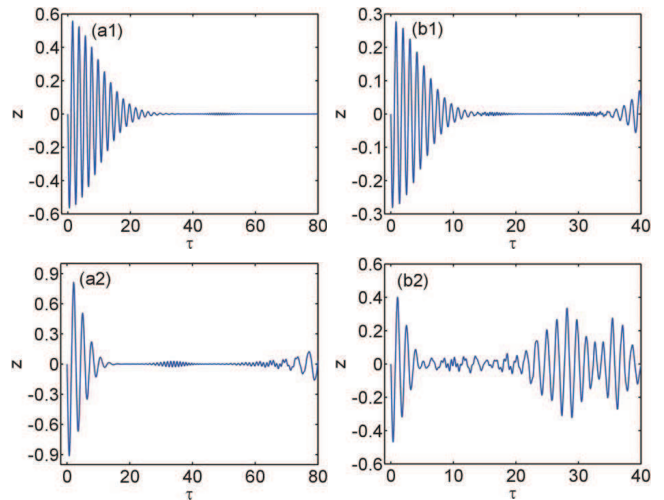


FIG. 6: (color online) Quantum quench dynamics of the system for repulsive interatomic interactions by suddenly changing the Peierls phase of the DW potential, where the initial state is the ground state of the DW system with $\theta = 0$. (a1) $U_0 = 2$, $\theta = \pi/3$, (a2) $U_0 = 2$, $\theta = 2\pi/3$, (b1) $U_0 = 10$, $\theta = \pi/3$, and (b2) $U_0 = 10$, $\theta = 2\pi/3$. The other parameters are $N = 50$, $U_2/U_0 = 0.002$, and $\mu = 0$. Here the horizontal ordinate τ is in units of \hbar/J .

value of the oscillation amplitudes becomes larger, which is similar to the case of repulsive interactions. In addition, we find that the population difference keeps zero in the case of $\theta = \pi$ as shown in figure 7(a3). This point can be understood because for the weak attractive interaction of $U_0 = -2$ the ground state of the DW system is still symmetric, which is similar to the case of repulsive interactions. For strong attractive interaction and $\theta = 0$, the ground state of the DW system is a quantum self-trapping state with a large population difference, i.e., the atoms are self-trapped in a single trap (e.g., the right trap) of the DW potential. Once the Hamiltonian is quenched due to the sudden change of the Peierls phase θ , the oscillation gradually decays and the population difference eventually resumes its original value $z = -0.991$, which can be seen in figures 7(b1)-7(b3). In the case of $0 < \theta \leq \pi$, a larger Peierls phase θ implies a higher oscillation amplitude. We expect that the effect of the Peierls phase on the quench dynamics of the DW system can be observed and tested in the future experiments.

VI. CONCLUSION

In summary, we have applied a full quantum-mechanical procedure to investigate the properties of the stationary states of BECs in a DW potential and the quantum dynamics of the system with a maximum initial population difference. At the same time, the quantum quench dynamics of the system is studied by suddenly changing the Peierls phase of the DW potential.

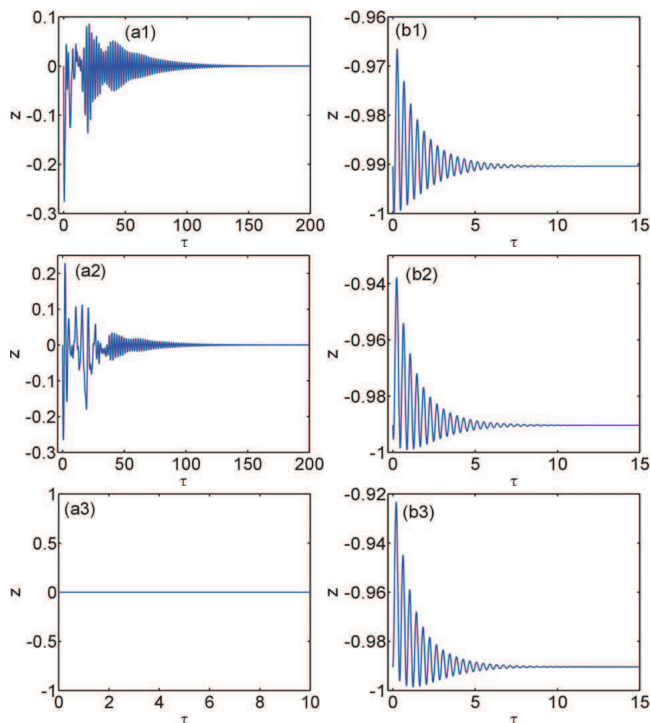


FIG. 7: (color online) Quantum quench dynamics of the system for attractive interatomic interactions by suddenly changing the Peierls phase of the DW potential, where the initial state is the ground state of the DW system with $\theta = 0$. (a1) $U_0 = -2$, $\theta = \pi/3$, (a2) $U_0 = -2$, $\theta = 2\pi/3$, (a3) $U_0 = -2$, $\theta = \pi$, (b1) $U_0 = -8$, $\theta = \pi/3$, (b2) $U_0 = -8$, $\theta = 2\pi/3$, and (b3) $U_0 = -8$, $\theta = \pi$. The other parameters are $N = 50$, $U_2/U_0 = 0.002$, and $\mu = 0$. Here the horizontal ordinate τ is in units of \hbar/J .

We show that the pair tunneling influences significantly the density profiles and energy spectrums of the stationary states especially for the cases of medium or strong interatomic interactions. With the increase of the ratio between the pair tunneling strength and the single-particle tunneling strength, the eigenstates of the Hamiltonian become pair degenerate and the corresponding energy levels ultimately keep almost constant. In addition, it is shown that in the case of weak repulsion the strong pair tunneling sustains a quantum self-trapping for the quantum dynamics of the DW system with a maximum initial population difference while in the case of large repulsion the strong pair tunneling tends to destroy the self-trapping effect. By contrast, for the case of attractive interactions the strong pair tunneling tends to eliminate the Josephson oscillations and the quantum self-trapping irrespective of the interaction strength. Moreover, when the DW system is quenched, the population difference shows evident oscillation behaviors for most cases. The maximum amplitude of the oscillation is directly relevant to the value of the Peierls phase. These properties are remarkably different from those in a conventional DW BEC with no pair tunneling, which allows to be observed and tested in the future experiments.

Acknowledgments

We thank Biao Wu, Ming Gong, and Chunlei Qu for helpful discussions and comments. This work is supported by NSFC (Grants No. 11475144 and No. 11304270), NSF of Hebei Province (Grant No. A2015203037), and Ph.D. foundation of Yanshan University (Grant No. B846).

-
- [1] Leggett A J 2001 *Rev. Mod. Phys.* **73** 307
 - [2] Ueda M 2010 *Fundamentals and New Frontiers of Bose-Einstein Condensation* (Singapore: World Scientific)
 - [3] Smerzi A, Fantoni S, Giovanazzi S and Shenoy S R 1997 *Phys. Rev. Lett.* **79** 4950
 - [4] Milburn G J, Corney J, Wright E M and Walls D F 1997 *Phys. Rev. A* **55** 4318
 - [5] Pu H, Zhang W and Meystre P 2002 *Phys. Rev. Lett.* **89** 090401
 - [6] Albiez M, Gati R, Fölling J, Hunsmann S, Cristiani M and Oberthaler M K 2005 *Phys. Rev. Lett.* **95** 010402
 - [7] Ananikian D and Bergeman T 2006 *Phys. Rev. A* **73** 013604
 - [8] Wen L H and Li J H 2007 *Phys. Lett. A* **369** 307
 - [9] Shchesnovich V S and Trippenbach M 2008 *Phys. Rev. A* **78** 023611
 - [10] Adhikari S K, Lu H and Pu H 2009 *Phys. Rev. A* **80** 063607
 - [11] Julia-Diaz B, Dagnino D, Lewenstein M, Martorell J and Polls A 2010 *Phys. Rev. A* **81** 023615
 - [12] Gillet J, Garcia-March M A, Busch Th and Sols F 2014 *Phys. Rev. A* **89** 023614
 - [13] Gati R and Oberthaler M K 2007 *J. Phys. B* **40** R61
 - [14] Edmonds M J, Valiente M and Öhberg P 2013 *J. Phys. B* **46** 134013
 - [15] Spekkens R W and Sipe J E 1999 *Phys. Rev. A* **59** 3868
 - [16] Julia-Diaz B, Martorell J and Polls A 2010 *Phys. Rev. A* **81** 063625
 - [17] Wu Y and Yang X 2003 *Phys. Rev. A* **68** 013608
 - [18] Carr L D, Dounas-Frazer D R and Garcia-March M A 2010 *EPL* **90** 10005
 - [19] Mahmud K W, Perry H and Reinhardt W P 2005 *Phys. Rev. A* **71** 023615
 - [20] Wen L H, Xiong H W and Wu B 2010 *Phys. Rev. A* **82** 053627
 - [21] Wen L H and Luo X B 2012 *Laser Phys. Lett.* **9** 618
 - [22] Garcia-March M A and Carr L D 2015 *Phys. Rev. A* **91** 033626
 - [23] Carvalho D W S, Foerster A and Gusmão M A 2015 *Phys. Rev. A* **91** 033608
 - [24] Murmann S, Bergschneider A, Klinkhamer V M, Zürn G, Lompe T and Jochim S 2015 *Phys. Rev. Lett.* **114** 080402

- [25] Malomed B A 2015 *Nat. Photonics* **9** 287
- [26] Fölling S, Trotzky S, Cheinet P, Feld M, Saers R, Widera A, Müller T and Bloch I 2007 *Nature (London)* **448** 1029
- [27] Zöllner S, Meyer H-D and Schmelcher P 2008 *Phys. Rev. Lett.* **100** 040401
- [28] Liang J-Q, Liu J-L, Li W-D and Li Z-J 2009 *Phys. Rev. A* **79** 033617
- [29] Zhu Q, Zhang Q and Wu B 2015 *J. Phys. B* **48** 045301
- [30] Dalibard J, Gerbier F, Juzeliūnas G and Öhberg P 2011 *Rev. Mod. Phys.* **83** 1523
- [31] Jiménez-García K, LeBlanc L J, Williams R A, Beeler M C, Perry A R and Spielman I B 2012 *Phys. Rev. Lett.* **108** 225303
- [32] Struck J, Ölschläger C, Weinberg M, Hauke P, Simonet J, Eckardt A, Lewenstein M, Sengstock K and Windpassinger P 2012 *Phys. Rev. Lett.* **108** 225304
- [33] Zheng W and Zhai H 2014 *Phys. Rev. A* **89** 061603(R)
- [34] Greschner S, Sun G, Poletti D and Santos L 2014 *Phys. Rev. Lett.* **113** 215303
- [35] Qu C, Hamner C, Gong M, Zhang C and Engels P 2013 *Phys. Rev. A* **88** 021604(R)
- [36] Dong Y, Dong L, Gong M and Pu H 2015 *Nat. Commun.* **6** 6103
- [37] Jaksch D, Bruder C, Cirac J I, Gardiner C W and Zoller P 1998 *Phys. Rev. Lett.* **81** 3108
- [38] Bader P and Fischer U R 2009 *Phys. Rev. Lett.* **103** 060402
- [39] Dutta O, Gajda M, Hauke P, Lewenstein M, Lühmann D -S, Malomed B A, Sowiński T and Zakrzewski J 2015 *Rep. Prog. Phys.* **78** 066001
- [40] Greiner M, Mandel O, Esslinger T, Hänsch T W and Bloch I 2002 *Nature (London)* **415** 39